Chapter 4

Intramolecular Crosslinking of Helical Folds: A Novel Approach to Organic Nanotubes

The tubular secondary structure of a folded helical polymer - a poly(*m*-phenylene ethynylene) derivative, synthesized via our A_2+BB' polycondensation method, is stabilized by intramolecular cross-linking of cinnamate moieties through topchemically controlled photodimerization. This approach should enable the generation of organic nanotubes with controlled dimensions and surface functionality that constitute attractive building blocks for functional nanostructures.

Part of this work has been published: (a) *Angew. Chem.* **2003**, *115*, 6203; *Angew. Chem. Int. Ed.* **2003,** *42*, 6021. (b) *Synth. Met.* **2004**, *147*, 37.

Introduction

The design and synthesis of hollow tubular, functional nanostructures of controlled dimensions and defined surface chemistry remains a challenging and attractive target in both bio- and nanosciences.[1,2] Integration of these molecular building blocks into larger, more complex structures using self-assembly or manipulation promises potential applications in several areas including chemical and charge transport as well as sensing and catalysis.

Inspired by natural design concepts, several molecular based approaches to obtain organic nanotubes have been developed and promise a superior control over structure and local functionality.[3, 4] Most of the strategies explored thus far have taken advantage of a combination of covalent and non-covalent syntheses based on various structural motifs including hollow or self-assembled helices, stacked macrocycles and rosettes, cylindrical micelles and rolled bilayer sheets. (Figure 1)

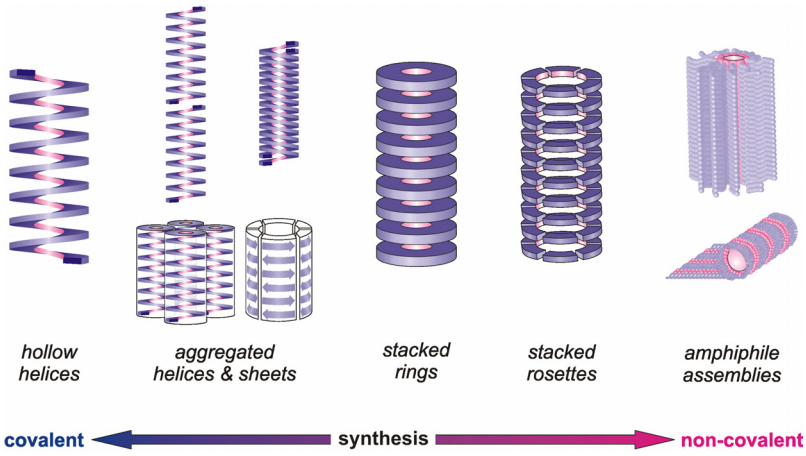

Figure 1. General strategies for the design of organic nanotubes based on hollow helical scaffolds and their self-assembly, stacks of macrocycles and rosettes, as well as cylindrical micelles and rolled bilayer sheets.

We describe a conceptually new approach (Figure 2) to generate organic nanotubes on the basis of intramolecularly crosslinked, helically folded polymers.[5] Our concept (Figure 2) involves polymerization of an appropriately functionalized monomer containing folding promoting features as well as crosslinking units. The formed polymer strand (primary structure) is able to adopt a helical conformation (secondary structure), in which reactive groups are oriented within close proximity to allow for subsequent covalent stabilization of the tubular nanoobject. Subsequent inner and outer postfunctionalization yields nanochannels or insulated nanowires with defined surface functionality and controlled dimension. These advanced nanoobjects are potentially interesting building blocks for the construction of new materials and devices.

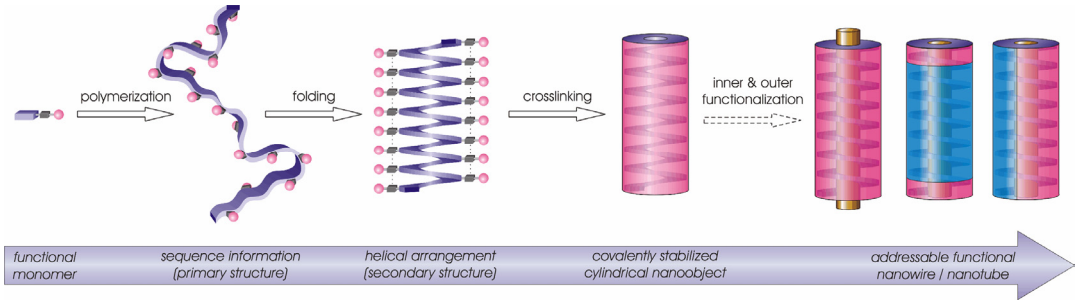

Figure 2. Formation of organic nanotubes by the intramolecular cross-linking of helically folded polymer backbones. Polymerization of a functional monomer carrying both solvophilic (magenta) and cross-linking groups (gray) generates a polymer strand that folds into a helical conformation that is subsequently stabilized by covalent cross-linking using adjacent reactive groups.

Our approach takes advantage of the power of covalent chemistry to yield a defined oligomer/polymer sequence and enhance the object's stability by crosslinking, while utilizing non-covalent interactions to drive the formation of the helical structure without defects. It should be noted that in principle our strategy allows for unprecedented control over surface functionality as well as length control. Furthermore, the inherent chirality of the helical scaffold should provide the nanotubes with additional advantageous properties.

Choice of the Backbone

The polymer backbone of choice has to contain all necessary information and functionality in order to: (i) fold in a reversible fashion into a hollow helical structure in which the non-neighboring crosslinking groups are located in close proximity, (ii) specific residues are exposed at the inner and outer surfaces to allow for postfunctionalization, (iii) all chemical processes can be carried out independently, i.e. they are orthogonal to one another. These stringent requirements exclude most known helical foldamers[6] and polymers[7,8] since most of these compounds do not contain an inner void and their high pitch hinders efficient crosslinking due to large side chain separation. On the contrary, Moore's amphiphilic oligo(*meta*-phenylene ethynylene)s[9] offer several advantages since they contain a significant inner void (assuming a 6-helix[10] yields an available inner cavity measuring approximately 0.7 nm in diameter), allow for the introduction of multiple crosslinks per turn, position the reactive groups in close proximity (π,π-stacking distance of neighboring units in adjacent turns), and exhibit a well-characterized conformational behavior that can easily be monitored using UV/vis absorption and fluorescence

spectroscopies. Therefore, amphiphilic poly(*meta*- ethynylene)s[11] were chosen as the backbone in our initial experiments while the reactive groups were incorporated as cinnamates to utilize [2+2]photodimerization reactions for intramolecular crosslinking.

Backbone Synthesis

The diiodocinnamate monomer **2** was synthesized from 3,5-diiodobenzaldehyde[12] in two steps involving a Knoevenagel-type condensation followed by esterification with triethylene glycol monomethyl ether. (Scheme 1)

Scheme 1

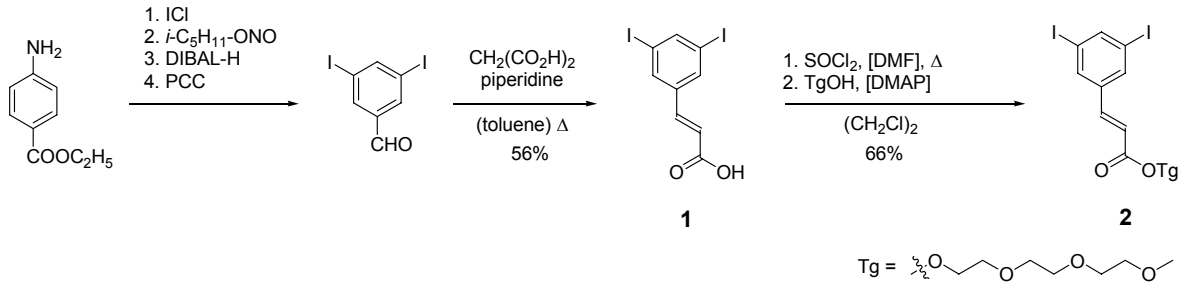

We employed our recently developed A_2+BB' polycondensation route[13] (Chapter 2) to prepare poly(*m*-phenylene ethynylene) **3** (Scheme 2) having a respectable number average degree of polymerization (DP ~ 60) and a typical polydispersity index (PDI = 1.3).

Scheme 2

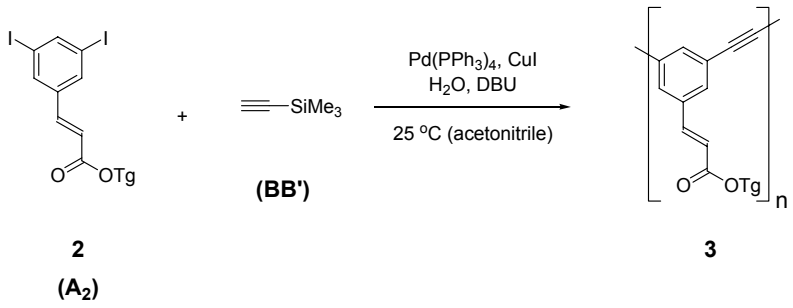

Both UV/vis as well as fluorescence spectroscopy in THF at 40 °C (GPC conditions) suggest major population of the helical conformation (see also Figure 9) and therefore the molecular weight determined by GPC most likely represents a lower limit. Most importantly, comparison of the ^{13}C NMR spectra of **3** with literature values of diacetylene oligomers almost exactly resembling the investigated polymer repeat units[14] clearly shows the absence of detrimental diyne defects in the polymers (**3**) prepared by our method.(Fig 3)

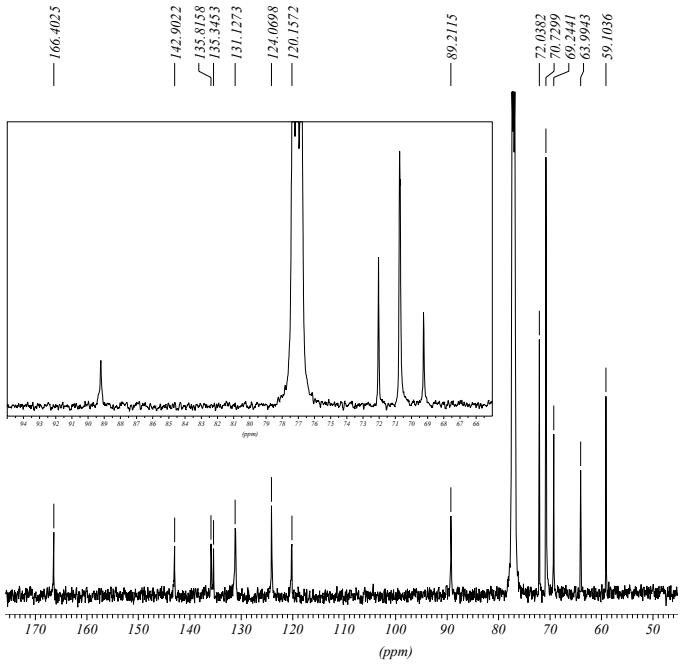

Figure 3. ^{13}C-NMR spectrum of polymer **3** (500 MHz, $CDCl_3$, 25 ^{o}C). The inset shows the region of potential diyne defects.

Backbone Folding

UV/vis spectroscopy is a good tool to identify the helical conformation of poly(*m*-phenylene ethynylene)s. In polar solvents, absorption from repeat units adapting a *cisoid*-conformation is observed while in denaturing solvents the absorption spectra are comprised of two bands at 292 and 312 nm representing *cisoid*- and *transoid*- conformations, respectively.[9] The conformational transition can be seen by addition of the denaturing solvent, i.e. $CHCl_3$, to the folding promoting solvent, i.e. CH_3CN. Hypsochromism of the 312 nm band indicates the conformational change to a compact helical structure (Figure 4).

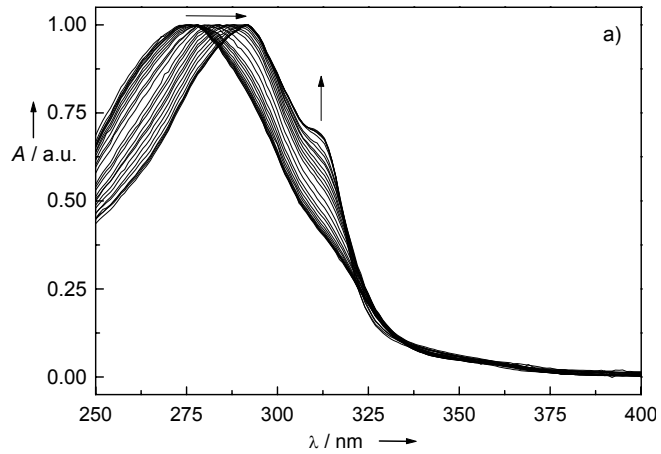

Figure 4. UV-visible absorption spectra of polymer **3** in acetonitrile with increasing chloroform content (100% $CH_3CN \rightarrow$ 100% $CHCl_3$). The spectra, measured at approximately the same concentration, have been normalized with respect to their maximum intensity.

Fluorescence spectroscopy is an alternative tool study the conformational transition in these foldamers. In the unfolded state, emission arises from isolated (cross-conjugated) repeat units while "pseudoexcimer"-like emission from stacked repeat units is associated with the helical conformation (Figure 5).[15]

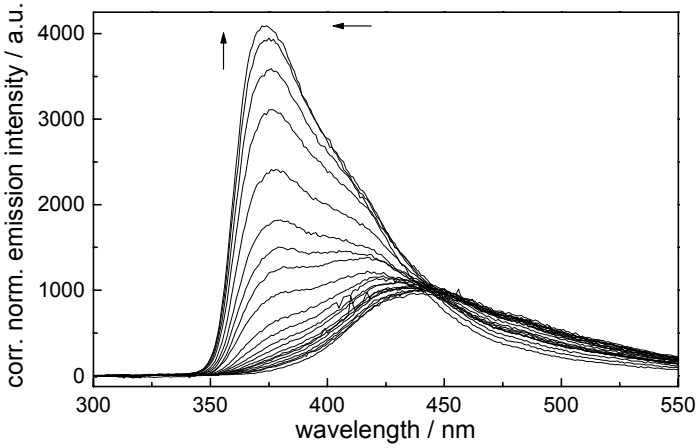

Figure 5. Fluorescence emission spectra of polymer **3** in acetonitrile with increasing chloroform content (100% $CH_3CN \rightarrow$ 100% $CHCl_3$). The spectra, measured at approximately the same concentration, have been corrected and normalized with respect to the optical density at the excitation wavelength OD_{290nm}.

Solvent denaturation experiments on polymer **3** reveal a typical sigmoidal, i.e. cooperative, folding behavior (see Figure 9). When compared to shorter oligomers of related

structure,[9, 10] similar solvent titration curves having a slightly shifted transition point indicating a more stable helix as predicted by the helix-coil model[16] are observed. However for reasons yet unknown, the transition does not appear to be sharpened.

Backbone Crosslinking

In order to lock the helical structure, multiple dimeric crosslinks were introduced via topochemically controlled [2+2]photodimerization events between stacking cinnamate moieties.[17, 18] For this purpose, polymer **3** was irradiated under high dilution conditions in the folding promoting solvent acetonitrile (Scheme 3).

Scheme 3

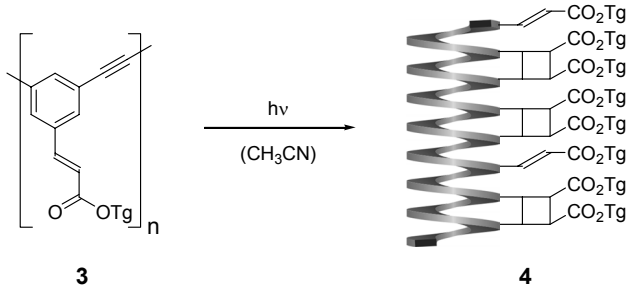

Monitoring the smoothly decreasing UV/vis absorbance (Figure 6) and the corresponding extinction difference analysis (Figure 7) indicate clean photoconversion of the cinnamate moieties.

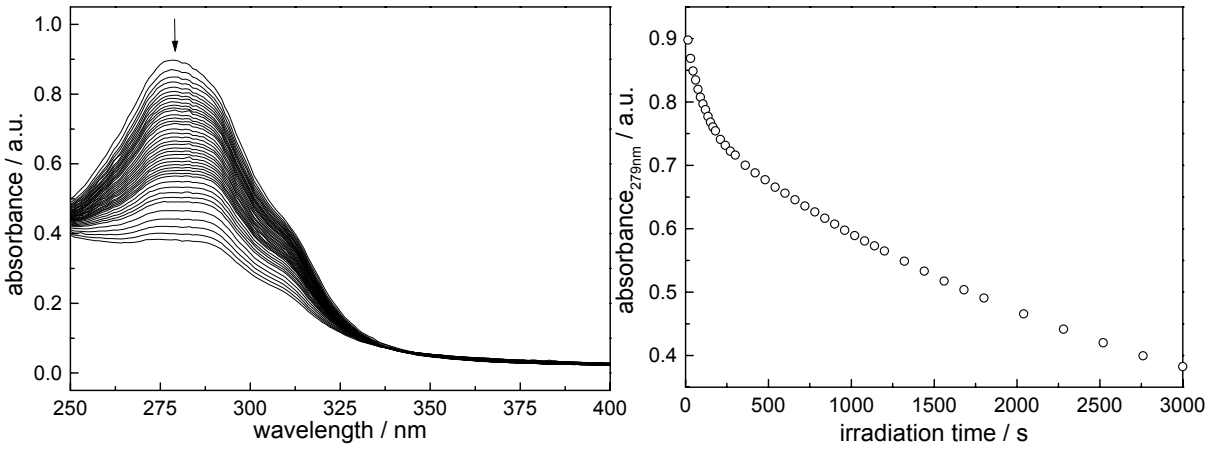

Figure 6. UV-visible absorption spectra of polymer **2** during irradiation (~ $7 \cdot 10^{-6}$ M in CH_3CN) (left). Plot of abs_{279nm} as a function of irradiation time (right).

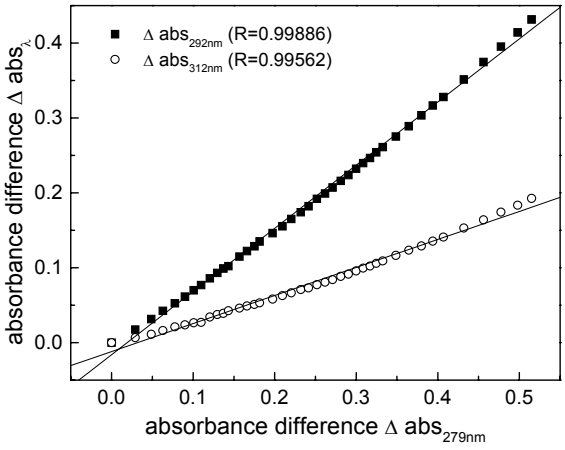

Figure 7. Extinction difference diagram for irradiation of **2** showing both Δabs_{292nm} and Δabs_{312nm} as a function of Δabs_{279nm}

After 20 minutes of irradiation, the resulting crosslinked polymer **4** was again subjected to an UV/vis titration experiment (Figures 8 and 9).

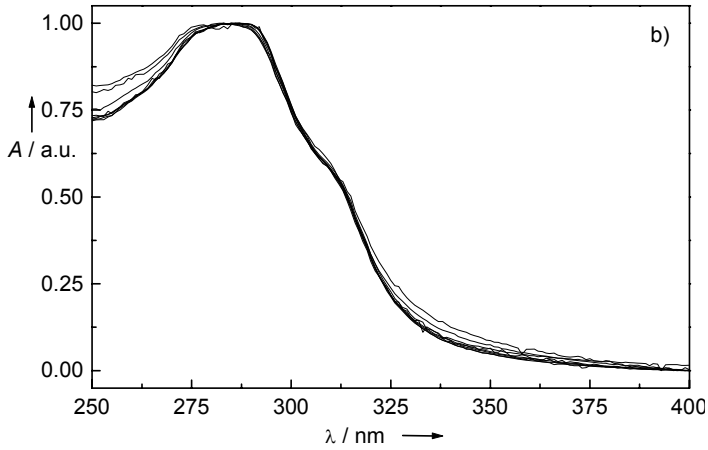

Figure 8. UV-visible absorption spectra of: a) polymer **3** and b) crosslinked polymer **4** in acetonitrile with increasing chloroform content (100% CH_3CN → 100% $CHCl_3$). The spectra, measured at approximately the same concentration, have been normalized with respect to their maximum intensity.

No significant spectral changes were observed with increasing amount of the denaturant chloroform[19] thereby clearly demonstrating the locked helical conformation.

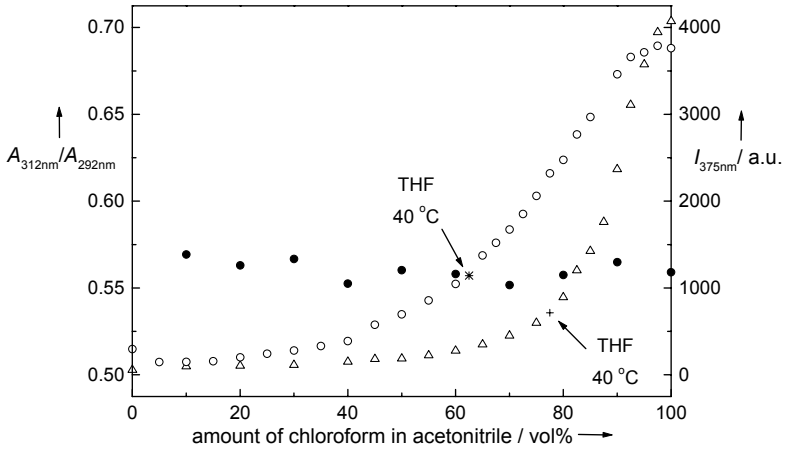

Figure 9. Plots of UV/vis absorbance ratio (abs_{312nm}/abs_{292nm}) and normalized fluorescence intensity (I_{375nm}), respectively, as a function of the volume percent chloroform in acetonitrile (25 °C): UV/vis of **3** (○), fluorescence of **3** (Δ), UV/vis of **4** (●). Also shown: UV/vis of **3** in THF at 40 °C (*) and fluorescence of **3** in THF at 40 °C (+).

The slightly higher absorbance ratio (abs_{312nm}/abs_{292nm}) (Figure 9) is attributed to some degree of structural reorganization during crosslinking as independently supported by the fluorescence spectrum of **4** in chloroform (Figure 10). While the almost negligible emission band (Figure 10 inset) is reminiscent of the folded "pseudoexcimer" **3**, the much lower emission intensity can be explained by the diminished π,π-overlap in **4** due to geometrical changes introduced by photodimerization.

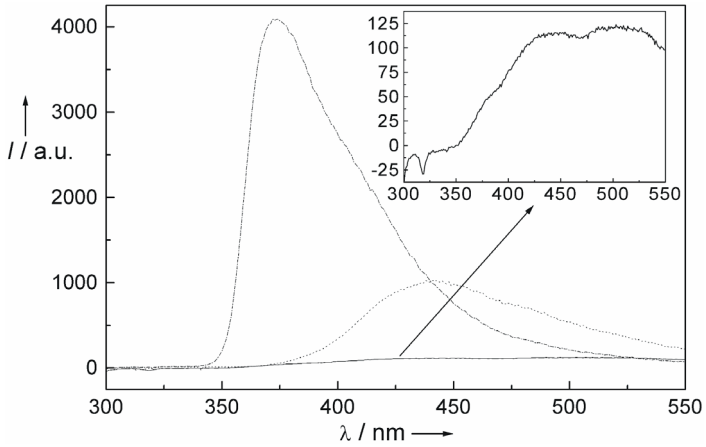

Figure 10. Corrected normalized fluorescence spectra of amphiphilic poly(*m*-phenylene ethynylene) before (**2**) and after (**3**) irradiation (25 °C): **3** in $CHCl_3$ (– · – · –), **3** in CH_3CN (· · · · ·), **4** in $CHCl_3$ (———). The inset shows a magnification of **4** in $CHCl_3$.

Molecular mechanics calculations point to the introduction of a considerable tilt angle of ~ 30° while the distance between the π-systems remains constant during the crosslinking process (Figure 11).

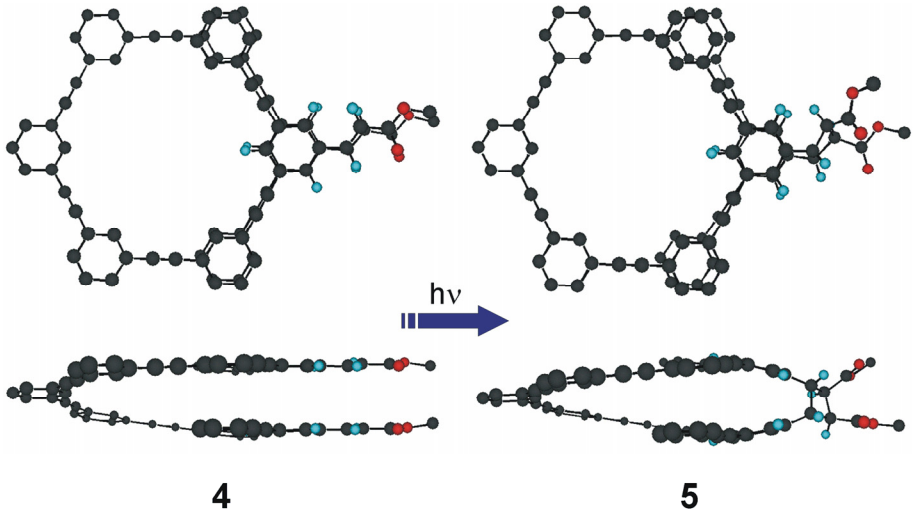

Figure 11. Topochemical crosslinking control: (a) MM2 optimized molecular models of two π,π-stacking crosslinking units in **3** showing one parallel, stacked cinnamate pair with a 3.4 Å distance before irradiation (top) and its resulting β-truxinate (syn head-head photodimer) after irradiation still exhibiting a 3.4 Å distance between the centers of the phenyl rings that are however tilted by 30.5° (bottom). For clarity, the side chains and hydrogen atoms of the helical backbone have been omitted.

In accordance with the topochemical principle,[18] the helical structure should favor the formation of β-truxinates, i.e. *syn* head-head photodimers, since they introduce the least conformational changes during the crosslinking event. Structural evidence for the proposed stereochemistry of β-truxinates arises from NMR spectroscopy (Figure 12) due to the diagnostic doublet at δ = 4.0 ppm.[21] In addition, the up-field shifted signal of the residual vinyl protons provides additional support for the locked helical structure[21] and allows a rough estimation of the degree of crosslinking amounting to ca. 20-30 %, which is in reasonable agreement with the UV/vis absorption decrease during the course of irradiation.

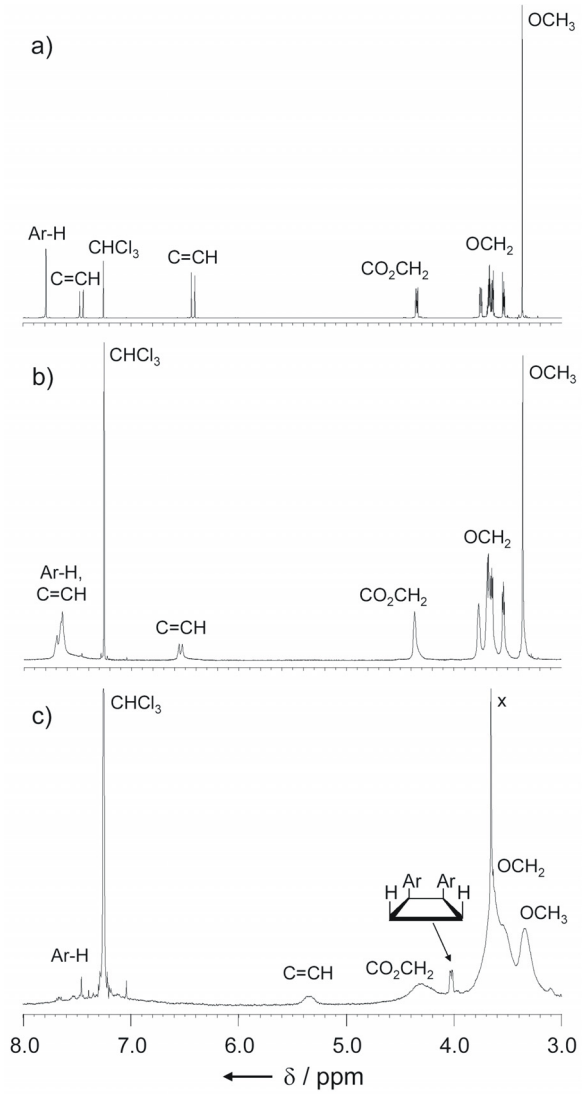

Figure 12. ^{1}H NMR spectral comparison ($CDCl_3$, 23 ± 2 °C): a) monomer **1**, b) polymer **2**, and c) polymer **3** (after 20 min irradiation period).

As expected, GPC analysis shows that short irradiation times favor formation of mainly intramolecularly crosslinked polymers, while extensive irradiation leads to additional intermolecular crosslinking (Figure 13). Performing the crosslinking reaction in a denaturant such as chloroform, a polymer with high degree of intermolecular crosslinks and transoid conformations was formed

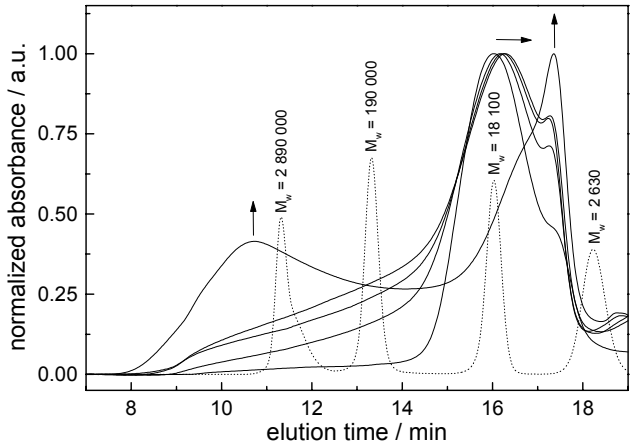

Figure 13. GPC traces for irradiation of polymer **3** in CH_3CN at 25 ^oC (curves correspond to t = 0, 5, 10, 20, 120 min, polystyrene standard used for calibration are shown in dotted lines).

Conclusions

We have shown the covalent stabilization of a hollow helical conformation and therefore demonstrate the feasibility of our novel approach to organic nanotubes (Figure 1). Utilizing this concept, organic nanotubes of controlled dimensions as well as specific local surface functionality should ultimately be realized. Work in progress to improve this initial system involves the use of helical backbones accessible via living/controlled polymerization (length control) and utilization of polymeric instead of dimeric crosslinking reactions.

Experimental

General Methods. 3,5-Diiodobenzaldehyde was prepared from ethyl 4-aminobenzoate in a four step sequence involving iodination, deamination, reduction followed by oxidation as described in the literature.[12] All other chemicals were commercial and used as received. THF and acetonitrile were distilled prior to use under N_2 atmosphere over sodium/benzophenone ketyl and calcium hydride, respectively. Column chromatography was carried out with 130-400 mesh silica gel. NMR spectra were recorded on Bruker AB 250 (250.1 and 62.9 MHz for ^1H and ^{13}C, respectively) and AC500 as well as Delta JEOL Eclipse 500 (500 and 126 MHz for ^1H and ^{13}C, respectively) spectrometers at 23 ± 2 ^oC using residual protonated solvent signal as internal standard (^1H: $\delta(CHCl_3)$ = 7.24 ppm, δ(DMSO) = 2.49, $\delta(CH_3CN)$ = 1.94 ppm and ^{13}C: $\delta(CHCl_3)$ = 77.0 ppm, δ(DMSO) = 39.7 ppm). Mass spectrometry was performed on Perkin-Elmer Varian Type MAT 771 and CH6 (EI), Type CH5DF (FAB), or Bruker Reflex with 337 nm laser excitation (MALDI-TOF) instruments. Elemental analyses were performed on a Perkin-Elmer EA 240. GPC measurements were performed on a Waters 515 HPLC pump-GPC system equipped with a Waters 2487 UV detector (254 nm detection wavelength) using THF as the mobile phase at 40 ^oC and a flow rate of 1 mL/min. The samples were separated through Waters Styragel HR1 or HR3 columns with 5 μm bead sizes. The columns were calibrated with several narrow polydispersity polystyrene samples and toluene served as internal standard. The HPLC system consisted of a Knaur Eurosphere 7μm C18, 4·120 mm silica gel column and UV-detection at 254 nm with an eluent flow of 1 mL/min.

Optical spectroscopy. UV/visible absorption and fluorescence emission/excitation spectra were recorded in various solvents of spectroscopic grade using quartz cuvettes of 1 cm path length on a Cary 50 Spectrophotometer and a Cary Eclipse Fluorescence Spectrophotometer, respectively, both equipped with Peltier thermostated cell holders (ΔT = ± 0.05 ^oC). Unless stated otherwise, all experiments were carried out at 25 ± 0.05 ^oC. For fluorescence measurements, the samples were not degassed since comparison of degassed with non-degassed solutions did not show measurable differences within the error of the experiment. The samples were excited at λ_{exc} = 290 nm, slit widths were set to 2.5 nm bandpass for excitation and 5 nm bandpass for emission. Fluorescence spectra were corrected for variations in photomultiplier response over wavelength using correction curves generated on the instrument. For titration experiments, stock solutions in

$CHCl_3$ and CH_3CN with optical densities OD(λ_{max}) ~ 0.8 for UV-visible absorption and OD(λ_{max}) ~ 0.1 for fluorescence measurements were used to prepare samples with varying solvent composition. The corrected fluorescence spectra were normalized by the exact OD_{290nm}.

Irradiation of Poly(*m*-aryleneethynylene) 3. Preparative irradiations were performed using a Philips HPK 125 W high-pressure mercury lamp equipped with a water-cooled photoreactor of Duran® (pyrex) glass ($\lambda_{5\%T}$ = 316 nm). The solutions (10 mg polymer **3** / 100 mL CH_3CN, ~ $7 \cdot 10^{-6}$ M) were degassed with nitrogen for 10 min, continuously irradiated, and samples for GPC and UV/vis taken at given time intervals. For ^{1}H NMR spectra, the solvent was evaporated at a given time, the sample thoroughly dried on a vacuum pump, and redissolved in $CDCl_3$.

3,5-Diiodocinnamic acid (1). 3,5-Diiodobenzaldehyde (1.07 g, 3 mmol), malonic acid (0.31 g, 3 mmol), piperidine (1 mL), DMF (8 mL), glacial acetic acid (1 mL), and acetic anhydride (1 mL) were suspended in toluene (10 mL) and heated overnight at 120 °C. Then, water (30 mL) was added and it was refluxed for 1 h. The formed white solid was isolated by filtration and washed with water to afford the crude acid that can be further purified by recrystallization from ethanol furnishing 0.70 g of a white solid (56% yield). ^{1}H NMR (250 MHz, DMSO-d_6, 23±2 ^{o}C): δ 8.08 (broad s, 3 H, Ar-H), 7.42 (d, ^3J (H,H) = 16.4 Hz, 1 H, C=CH-), 6.61 (d, ^3J (H,H) = 16.4 Hz, 1 H, C=CH-); ^{13}C NMR (125 MHz, DMSO-d_6, 23±2 ^{o}C): δ 172.17, 150.47, 145.86, 143.58, 140.95, 127.20, 101.57; EI-MS (80 eV, 100 °C): *m/z* = 400.0 (calcd 399.9 for $C_9H_6I_2O_2^+$); Anal. C: 26.87, H: 1.19 (calcd C: 27.03, H: 1.51).

2-[2-(2-methoxy-ethoxy)-ethoxy]-ethyl 3,5-diiodocinnamate (2). Crude acid **1** (4.60 g, ~ 11.5 mmol) was mixed with thionyl chloride (15 mL), 3 drops of DMF added, and it was heated at 60 ^{o}C for 2 h. Excess thionyl chloride was evaporated and the remaining compound dried on a vacuum pump for 3 h to afford the crude acid chloride as a light brownish solid. Triethylene glycol monomethyl ether (2.7 mL, 17.25 mmol), triethylamine (3.2 mL, 23.0 mmol), and 4-dimethylaminopyridine (DMAP; 0.14 g, 1.15 mmol) were dissolved in CH_2Cl_2 (10 mL), the solution cooled to 0 ^{o}C (ice bath), a solution of the acid chloride in CH_2Cl_2 (30 mL) slowly added over a period of 30 min, the resulting reaction mixture allowed to warm to rt and stirred overnight. Filtration followed by washing of the filtrate with sat. aqueous NH_4Cl and brine, drying over $MgSO_4$, evaporation of the solvent, and column chromatography (40 % ethyl acetate in hexane, R_f = 0.2) gave 4.136 g of the product as slightly yellow oil (~66% yield). ^{1}H NMR (500 MHz, $CDCl_3$, 23±2 ^{o}C): δ 8.01 (t, ^4J (H,H) = 1.5 Hz, 1 H, Ar-H), 7.77 (d, ^4J (H,H) = 1.5 Hz,

2 H, Ar-H), 7.44 (d, ^3J (H,H) = 16.0 Hz, 1 H, C=CH-), 6.40 (d, ^3J (H,H) = 16.0 Hz, 1 H, C=CH-), 4.33 (t, ^3J (H,H) = 4.8 Hz, 2 H, CO_2-CH_2), 3.74 (t, ^3J (H,H) = 4.8 Hz, 2 H, O-CH_2), 3.68-3.62 (m, 6 H, O-CH_2), 3.53 (t, ^3J (H,H) = 4.8 Hz, 2 H, O-CH_2), 3.35 (s, 3 H, O-CH_3); ^{13}C NMR (125 MHz, $CDCl_3$): δ 165.95, 146.30, 141.47, 138.08, 135.97, 120.53, 71.92, 70.62, 70.58, 69.09, 63.94, 59.04; EI-MS (80 eV, 150 °C): 546.1 (M^+, 21%), 501 (M-$C_2H_5O^+$, 6%), 427 (M-$C_5H_{11}O_3^+$, 100%), 383 (M-$C_7H_{15}O_4^+$, 80%), 256 (M-$C_5H_{11}O_3I^+$, 61%), EI-HRMS: *m*/*z* = 545.94333 (calcd 545.94000 for $C_{16}H_{20}O_5I_2^+$), 426.86577 (calcd 426.86920 for $C_{11}H_9O_2I_2^+$), 382.84455 (calcd 382.84299 for $C_9H_5OI_2^+$); Anal. C: 35.29, H: 3.39 (calcd C: 35.19, H: 3.69); HPLC (90% MeOH in H_2O, 1 mL/min): 99.0% peak area.

Poly(*m*-aryleneethynylene) 3. Monomer **2** (546 mg, 1 mmol), CuI (15 mg, 0.08 mmol), and $Pd(PPh_3)_4$ (69 mg, 0.06 mmol) were loaded in a flame dried 10 mL Schlenk tube, which was evacuated and refilled with argon. Dry and degassed acetonitrile (4 mL) was submitted to the tube via syringe, 1,8-diazabicyclo[5.4.0]undec-7-ene (DBU; 0.9 mL, 6 mmol) and trimethylsilylacetylene (TMSA; 142 μL, 1 mmol) were added immediately followed by addition of distilled H_2O (18 μL, 1 mmol). The tube was covered with aluminum foil and the reaction mixture was allowed to stir at rt for 3 d after which it was precipitated in ether (500 mL). The resulting polymer was redissolved in CH_2Cl_2 and passed through a short column of silica gel to give ~250 mg of **3** as a greyish powder (~79% yield). ^{1}H NMR (500 MHz, $CDCl_3$, 23±2 °C): δ 7.68-7.62 (broad m, 4 H, Ar-H, C=CH), 6.53 (broad d, ^3J (H,H) = 15.7 Hz, 1 H, C=CH), 4.35 (broad t, 2 H, CO_2-CH_2), 3.75 (broad t, 2 H, O-CH_2), 3.67-3.62 (broad m, 6 H, O-CH_2), 3.52 (broad t, 2 H, O-CH_2), 3.34 (broad s, 3 H, O-CH_3); ^{13}C NMR (125 MHz, $CDCl_3$): δ 166.40, 142.90, 135.82, 135.35, 131.13, 124.07, 120.16, 89.21, 77.04, 70.73, 69.24, 63.99, 59.10; IR (KBr): 3434, 2923, 2853, 1716, 1641, 1593, 1288, 1177, 1106 cm^{-1}; Anal. C: 69.91/69.52, H: 7.75/8.22 (calcd for $(C_{18}H_{20}O_5)_n$ C: 68.34, H: 6.37); GPC (THF, 40 °C): M_w = 24700, M_n = 18400, PDI (M_w/M_n)= 1.34; UV/vis ($CHCl_3$, 25 °C) λ_{max} (abs/conc) 292 nm (0.581/70.6·mg/L).

References

1 For a comprehensive review on organic nanotubes, consult: D. T. Bong, T. D. Clark, J. R. Granja, M. R. Ghadiri, *Angew. Chem.* **2001**, *113*, 1016; *Angew. Chem. Int. Ed.* **2001**, *40*, 988.

2 For a recent review on inorganic nanostructures, see: Y. Xia, P. Yang, Y. Sun, Y. Wu, B. Mayers, B. Gates, Y. Yin, F. Kim, H. Yan, *Adv. Mater.* **2003**, *15*, 353.

3 D. T. Bong, T. D. Clark, J. R. Granja, M. R. Ghadiri, *Angew. Chem. Int.Ed.* **2001**, *40*, 988.

4 S. Hecht, M. A. Balbo Block, C. Kaiser, and A. Khan, *Top. Curr. Chem*. **2005**, *245*, 89.

5 S. Hecht and A. Khan, *Angew. Chem. Int. Ed*. **2003**, *42*, 6021.

6 D. J. Hill, M. J. Mio, R. B. Prince, T. S. Hughes, and J. S. Moore, *Chem. Rev*. **2001**, *101*, 3893.

7 T. Nakano, Y. Okamoto, *Chem. Rev*. **2001**, *101*, 4013.

8 J. J. L. M. Cornelissen, A. E. Rowan, R. J. M. Nolte, N. A. J. M. Sommerdijk, *Chem. Rev*. **2001**, *101*, 4039.

9 J. C. Nelson, J. G. Saven, J. S. Moore, P. G. Wolynes, *Science*. **1997**, *277*, 1793.

10 Defined as a helix having 6 repeat units per turn as evidenced by ESR double spin labeling experiments: K. Matsuda, M. T. Stone, and J. S. Moore, *J. Am. Chem. Soc*. **2002,** *124*, 11836.

11 For a comprehensive review about poly(phenylene ethynylene)s, mostly of the *para*-type, consult: U. H. F. Bunz, *Chem. Rev*. **2000**, *100*, 1605.

12 F. Li, S. I. Yang, Y. Ciringh, J. Seth, C. H. Martin, D. L. Singh, D. Kim, R. R. Birge, D. F. Bocian, D. Holten, J. S. Lindsey, *J. Am. Chem. Soc*. **1998**, *120*, 10001.

13 A. Khan and S. Hecht, Chem. Commun. **2004**, 300.

14 Y. Tobe, N. Utsumi, K. Kawabata, A. Nagano, K. Adachi, S. Araki, M. Sonoda, K. Hirose, K. Naemura, *J. Am. Chem. Soc*. **2002**, *124*, 5350.

15 R. B. Prince, J. G. Saven, P. G. Wolynes, J. S. Moore, *J. Am. Chem. Soc*. **1999**, *121*, 3114.

16 B. H. Zimm, J. K. Bragg, *J. Chem. Phys*. **1959**, *31*, 526.

17 G. M. J. Schmidt, *Pure & Appl. Chem*. **1971**, *27*, 647.

18 V. Ramamurthy, K. Venkatesan, *Chem. Rev*. **1987**, *87*, 433.

19 D. J. Hill, J. S. Moore, *Proc. Nat. Acad. Sci*. **2002**, *99*, 5053.

20 D. A. Ben-Efraim, B. S. Green, *Tetrahedron*. **1974**, *302*, 357.

21 Moore and coworkers reported on strong up-field chemical shifts upon transition to the folded helical structure. See: S. Lahiri, J. L. Thompson, J. S. Moore, *J. Am. Chem. Soc*. **2000**, *122*, 11315.